Biointerface Research in Applied Chemistry
Open-Access Journal (ISSN: 2069-5837)

Article
Volume 16, Issue 1, 2026, 12
https://doi.org/10.33263/BRIAC161.012

Synthesis, Characterization, and Antioxidant/Antibacterial Activities of New Mono- and Bi-Nuclear Complexes of Zn(II), Cu(II), and Co(II) Based on the Ligand 4-(benzo[d]thiazol-2-yl)-N, N-dimethylaniline

Ibtissam Elaaraj [1,*], Oumayma Oulidi [1], Safae Er Raouan [2], Aziz Bouymajane [3], Asmae Nakkabi [1], Ibnsouda Koraichi Saad [2], Francesco Cacciola [4,*], Noureddine El Moualij [1], Mohammed Fahim [1]

1 Laboratory of Bioinorganic Chemistry, Molecular Materials and the Environment, Faculty of Sciences, Moulay Ismail University, Meknes, Kingdom of Morocco; asmaenakkabi@yahoo.fr (A.N); oumaymaoulidi@gmail.com (O.O.); bachelorchimies1@yahoo.fr (N.E.M.); mo.fahim@yahoo.fr (M.F);
2 Laboratory of Microbial Biotechnology and Bioactive Molecules, Sciences and Technologies Faculty, Sidi Mohamed Ben Abdellah University, B.P. 2202 Fez, Morocco; serraouan@gmail.com (S.E.R.); saad.ibnsouda@usmba.ac.ma (I.K.S.);
3 Team of Microbiology and Health, Laboratory of Chemistry-Biology Applied to the Environment, Moulay Ismail University, Faculty of Sciences, B.P. 11201 Zitoune Meknes, Morocco; azizbouymajane.01@gmail.com (A.B);
4 Messina Institute of Technology (MeIT), Department of Chemical, Biological, Pharmaceutical and Environmental Sciences, former Veterinary School, University of Messina, Messina, Italy
* Correspondence: ibtissamelaraaj.123@gmail.com (I.E.); cacciolaf@unime.it (F.C.).

Received: 1.10.2025; Accepted: 16.11.2025; Published: 15.02.2026

Abstract: New mono- and bimetallic copper, zinc, and cobalt complexes derived from the ligand 4-(benzo[d]thiazol-2-yl)-N, N-dimethylaniline (L) were successfully synthesized and characterized using UV-visible, FT-IR, 1H-NMR, 13C-NMR, mass spectrometry, and molar conductance measurements. The molar conductance data confirmed that all synthesized complexes are non-electrolytes. Spectroscopic analyses indicated that the ligand coordinates with the metal ions in a monodentate fashion through its nitrogen atom. The antioxidant activity of the ligand and its metal complexes was tested using the DPPH assay, revealing that complexation significantly enhanced radical scavenging ability. The Cu(II) complex exhibited the strongest activity with an IC_{50} value of 0.008 ± 0.005 mg/mL, followed by Co(II) (0.014 ± 0.003 mg/mL), Zn(II) (0.024 ± 0.007 mg/mL), and the free ligand (0.043 ± 0.004 mg/mL), compared to ascorbic acid (0.046 ± 0.003 mg/mL). Antibacterial screening using the well-diffusion method on agar demonstrated that the metal complexes had greater inhibitory activity than the free ligand, particularly against Staphylococcus aureus and Pseudomonas aeruginosa, with minimum inhibitory concentration (MIC) values ranging from 0.25 to 1.0 mg/mL. Overall, this study reports the successful synthesis and comprehensive characterization of benzothiazole-based Schiff base metal complexes with markedly improved antioxidant and antibacterial properties, highlighting their potential as promising candidates for further pharmacological investigations.

Keywords: ligand; mono- and bi-metallic; complex; DPPH; antioxidant activity; antibacterial activity.

1. Introduction

The synthesis of nitrogen-containing heterocycles in a simple and efficient manner has attracted considerable attention from researchers and industry [1]. Among these, benzothiazoles represent an important class of bicyclic heterocyclic compounds in which a benzene ring is fused with a five-membered thiazole ring containing nitrogen and sulfur atoms [2]. This structural ring occurs naturally in a wide range of marine and terrestrial compounds. The benzothiazole skeleton serves as the core of numerous bioactive heterocycles and natural products, exhibiting diverse physicochemical properties, including optical activity, coordination ability, and electron-accepting behavior [3]. In recent years, benzothiazole derivatives have been extensively investigated for their medicinal potential. Various studies have demonstrated their broad spectrum of biological activities, including anticancer [4], antitumor [5], antibacterial [6], antifungal [7], antidiabetic [8], antioxidant [9], and anti-inflammatory [10] properties. Several fluorine- or nitrogen-substituted benzothiazoles have been synthesized and shown to possess potent anti-inflammatory and antitumor activities [11].

Furthermore, the amino functionality of benzothiazole derivatives can be converted into an imine (Schiff base) group, yielding Schiff base ligands that display a wide range of pharmacological activities [12]. These compounds have recently been explored as potential therapeutic agents for the treatment of diseases related to carcinogenesis, atherogenesis, and aging in aerobic organisms [13]. Heterocyclic Schiff bases and their metal complexes constitute a fascinating area of research due to their rich chemical reactivity and diverse antimicrobial properties [14]. The growing interest in bioinorganic medicinal chemistry has further spurred research on interactions between transition-metal complexes and nucleic acids. In particular, copper(II) Schiff base complexes are known to interact strongly with DNA, either through intercalation or surface binding, and exhibit DNA cleavage activity via oxidative or hydrolytic pathways [15]. These complexes have been screened in various biological assays and shown to possess significant biological potential [16]. Moreover, copper(II) complexes containing Schiff base and auxiliary ligands often display superior antioxidant activity compared to their homoleptic (mono-ligand) counterparts [14].

Despite the large number of studies on Schiff base metal complexes, relatively few investigations have focused on benzothiazole-based systems that combine both antioxidant and antibacterial evaluations. Most previous reports have focused on simple benzothiazole derivatives or Schiff bases, without establishing a clear relationship between their spectroscopic characteristics and biological activities. In addition, only a limited number of studies have explored environmentally friendly synthetic approaches for the preparation of such compounds under catalyst-free conditions.

The aim of the present work is, therefore, the facile, clean, and environmentally benign synthesis of the ligand 4-(benzo[d]thiazol-2-yl)-N, N-dimethylaniline (L) through the condensation of heteroaromatic aldehydes with 2-aminothiophenol in the absence of a catalyst. Furthermore, the antioxidant potential of the free ligand and its corresponding Zn(II), Cu(II), and Co(II) complexes was evaluated. The newly synthesized metal complexes were structurally characterized by chemical ionization mass spectrometry, UV-visible spectroscopy, Fourier-transform infrared spectroscopy (FT-IR), and nuclear magnetic resonance (1H and 13C NMR). Their antioxidant activities were subsequently assessed using the DPPH free radical scavenging assay.

2. Materials and Methods

2.1. Chemicals.

All chemicals used in this work were analytical reagent (AR) grade and of the highest purity. The ligand (L) synthesis components were purchased from Sigma-Aldrich. Melting points were recorded in open capillaries in a Stuart Melting Point apparatus, SMP10. IR spectra of the compounds were recorded using KBr pellets on the FT-IR Fourier transform infrared FTIR TENSOR27 spectrometer. Electronic absorption spectra were obtained on a Perkin-Elmer Lambda 35 UV-Vis spectrophotometer. NMR1H spectra of Schiff bases in DMSO-d6 were recorded on a JEOL 500 MHz FT NMR System JNM-ECZ500R/S1 spectrometer. The molar conductances of the studied metal chelates were obtained using the JENWAY conductance bridge model 4070. High-resolution mass spectra (HRMS) were acquired by the electron boiling ionization (ESI) technique using a Bruker APEX-2 instrument.

2.2. Synthesis of of 4-(benzo[d]thiazol-2-yl)-N,N-dimethylaniline.

Ethanolic solution of 2-aminothiophenol (0.125 g, 1 mmol) was added dropwise to ethanolic solution of N, N-dimethylaminobenzaldehyde (0.149 g, 1 mmol) in a 1:1 molar ratio. The reaction mixture was refluxed with stirring for 3-5 h, and the reaction progress was followed by thin-layer chromatography (TLC). The solid product formed was separated by filtration and then purified by crystallization in ethanol. The yellow crystals were obtained after filtration, diethyl ether washing, and drying under vacuum (Scheme 1).

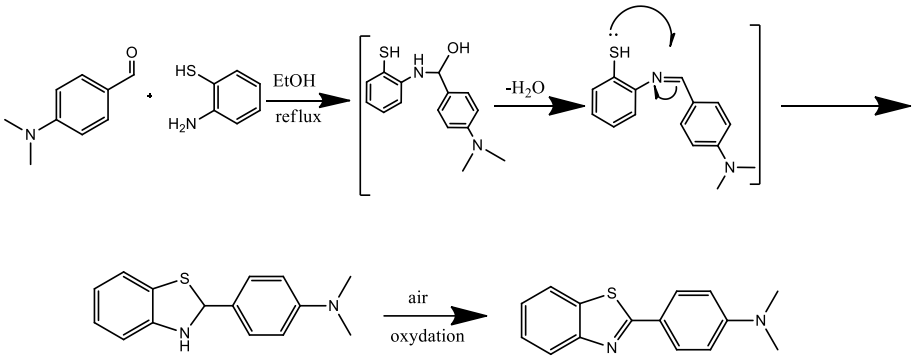

Scheme 1. Synthesis of ligand (L).

(L): solid yellow; R: 88%; m.p. 172°C; IR (KBr, cm^{-1}) ν: 3059-2918 C-H_{arom}, 1612 (N=C), 1556 (C=C), 1058 (C-N), 621(C-S); 1H NMR (500 MHz, DMSO-d6, ppm) δ:7.98-7.96 (d, J = 10 Hz, 1H Ar-H), 7.89-7.84 (m, 3H Ar-H), 7.44-7.41 (t, J=5 Hz, 1H Ar-H), 6.80-6.78 (d, J = 10 Hz, 2H Ar-H), 2.98 (s,6H N-CH_3), 7.33-7.30 (t, J = 5 Hz, 1H Ar-H); ^{13}C NMR (125 MHz, DMSO) δ: 168.39, 154.54-112.42 (Ar-C), 40,21(N-CH_3); MS (ESI) $[m/z]^+$=255.09; UV-Vis (DMSO): λ_{max} (nm) =309-355-403; Solubility: DMSO, MeOH, EtOH, DMF, $CHCl_3$.

2.3. Synthesis of the metal complexes ML_2Cl_2 (M=Cu; Zn) et $Co_2L_2(\mu\text{-}Cl)_2$

The complexes were prepared by condensation of an ethanolic solution (50 mL) of the metal salt MCl_2 (M=Cu; Zn) or $CoCl_2$ $6H_2O$ to an ethanolic solution (50 mL) of the ligand L with the stoichiometric ratios (1:2) metal: ligand (Scheme 2). The reaction mixture was heated at reflux for 2 h, and after cooling, the colored precipitate obtained was filtered, washed several times with cold ethanol, and then dried under vacuum.

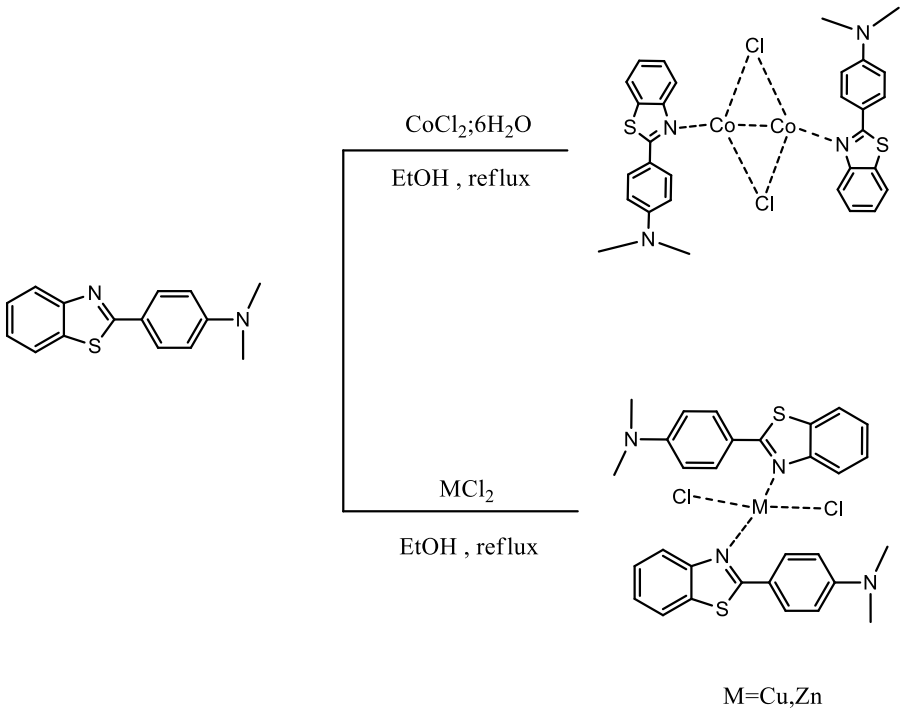

Scheme 2. Synthesis of complexes ML_2Cl_2 (M=Cu ; Zn) et $Co_2L_2(\mu\text{-}Cl)_2$.

ZnL_2Cl_2: solid yellow; R: 54%; m.p. >300°C; Λ(Scm^2mol^{-1}): 6.8; IR (KBr, cm^{-1}) ν: 3060-2959 C-Harom, 1588(N=C), 1572 (C=C), 1106 (C-N),600(C-S),452(M-N); ^1H NMR (500 MHz, DMSO-d6, ppm) δ:7.99-7.98 (d, J = 5Hz, 1H Ar-H), 7.89-7.84 (m, 3H Ar-H), 7.44-7.41 (t, J = 5 Hz, 1H Ar-H), 7.33-7.30 (t, J = 5 Hz, 1H Ar-H 6.79-6.77 (d, J = 10 Hz, 2H Ar-H), 2.97(s,6H N-CH_3); ^{13}C NMR (125 MHz, DMSO) δ: 168.40, 154.41-112.32 (Ar-C), 40.45(N-CH_3); MS (ESI) [*m/z*]$^+$=645.3; UV-Vis (DMSO): λ_{max} (nm) = 308-402;

Solubility: DMSO, DMF, $CHCl_3$

CuL_2Cl_2: solid black; R: 67%; m.p. >300°C; Λ(Scm^2mol^{-1}):9.9; IR (KBr, cm^{-1}) ν: 3042-2915 C-H_{arom}, 1609 (N=C), 1552 (C=C), 1066 (C-N), 619(C-S),473(M-N); 1H NMR (500 MHz, DMSO-d6, ppm) δ: 8.00-7.98 (d, J = 10Hz, 1H Ar-H), 7.89-7.84 (m, 3H Ar-H), 7.44-7.41 (t, J = 5 Hz, 1H Ar-H), 7.33-7.30 (t, J = 5 Hz, 1H Ar-H), 6.79-6.77 (d, J = 10 Hz, 2H Ar-H),2.97(s,6H N-CH_3); ^{13}CNMR (125 MHz, DMSO) δ: 167.76, 152.74-112.32 (Ar-C),40.44(N-CH_3); MS (ESI) [*m/z*]$^+$=644.11; UV-Vis (DMSO): max (nm) = 305-401-543; Solubility: DMSO, DMF, $CHCl_3$.

$Co_2L_2(\mu\text{-}Cl)_2$: solid green; R: 45%; m.p. >300°C; Λ(Scm^2mol^{-1}): 4.9; IR (KBr, cm^{-1}) ν: 3056-2924 C-H_{arom}, 1608 (N=C), 1559(C=C), 1064 (C-N), 620(C-S), 480(M-N); 1H NMR (500 MHz, DMSO-d6, ppm) δ: 8.01-7.99 (d, J = 10Hz, 1H Ar-H), 7.89-7.84 (m, 3H Ar-H), 7.44-7.41 (t, J = 5 Hz, 1H Ar-H), 7.33-7.30 (t, J = 5 Hz, 1H Ar-H), 6.80-6.78 (d, J = 10 Hz, 2H Ar-H),2.98(s,6H N-CH_3);)13CNMR (125 MHz, DMSO) δ: 167.34, 152.74-112.32 (Ar-C),40.48(N-CH_3); MS (ESI) [m/z]$^+$=697; UV-Vis (DMSO): max(nm) =399-338-601-692; Solubility: DMSO, DMF, $CHCl_3$

2.4. Antioxidant activity.

The stable 2,2-diphenyl-1-picrylhydrazyl (DPPH) radical scavenging assay is a widely used method for evaluating antioxidant activity, as it provides a simple, rapid, and reliable means of screening the radical scavenging potential of pure compounds or extracts [17]. DPPH

is a stable free radical capable of accepting an electron or hydrogen atom to form a diamagnetic molecule. In its radical form, DPPH exhibits a strong absorption band at 517 nm due to its unpaired electron. Upon reduction, this absorption decreases proportionally to the number of electrons or hydrogen atoms accepted, resulting in a visible color change from violet to pale yellow [18].

The assay was performed following the method described by Lopes-Lutz et al. [19], with minor modifications. Different concentrations of the ligand and its metal complexes (0.005-0.1 mg/mL) were prepared in dimethylformamide (DMF). For each sample, 1.0 mL of the test solution was mixed with 2.5 mL of DPPH solution (2.4 mg/100 mL in ethanol). A negative control was prepared by mixing 2.5 mL of the DPPH solution with 1.0 mL of pure methanol. After incubation for 30 minutes at room temperature, the absorbance of each sample was measured at 517 nm against the blank.

The radical-scavenging activity of each compound was determined from the decrease in absorbance, which reflects the ability of the sample to donate a hydrogen atom or an electron to neutralize the DPPH radical. Ascorbic acid was used as a reference antioxidant under the same experimental conditions.

All tests were performed in triplicate (n = 3), and the results are expressed as mean ± standard deviation (SD). The percentage inhibition (I%) of DPPH free radicals was calculated using Equation (1):

$$\%RSA = \frac{Ac-As}{Ac} \times 100 \qquad (1)$$

Ac: absorbance of the control (DPPH solution in the absence of the test compound).
As: absorbance in the presence of the test compound.

2.5. Antibacterial activity.

2.5.1. Microorganisms.

Antibacterial activities of the synthesized compounds were tested against Gram-positive and Gram-negative bacterial strains. Bacteria used were *Bacillus subtilis* ILP1428B, *Staphylococcus aureus* CIP543154 (Pasteur Institute Collection), Pseudomonas aeruginosa ATCC27653, and *Escherichia coli* CIP5412 (American Type Culture Collection).

2.5.2. Broth microdilution.

The microdilution test was used to determine the Minimum Inhibitory Concentration (MIC) in a 96-well microplate. Mueller Hinton Broth was supplemented with the emulsifier (1% (v/v) DMSO). Then, 50 µL of bacterial (10^6 CFU/mL) was deposited. Finally, bacterial growth was revealed by turning resazurin from purple to pink. The lowest inhibitory concentration of the compound solution corresponded to the lowest concentration that inhibited the reduction of blue resazurin dye into pink resorufin. MBC was determined by sub-culturing the contents of wells with concentrations above the MIC values onto LB agar plates and incubating them at 37°C for a further 24 hours [20].

3. Results and Discussions

3.1. Molar conductance measurements.

At room temperature, the molar conductance of 10^{-3} M solutions of the produced metal complexes in dimethylformamide (DMF) was measured. The newly made solutions had molar conductivity values between 4.9 to 9.9 $S \cdot cm^2 \cdot mol^{-1}$. These low values suggest that the chloride ions are coordinated to the central metal atom rather than existing as free ions in solution, indicating the non-electrolytic character of the metal complexes [21]. The solutions were found to be relatively neutral, and the complexes remained stable in solution.

According to the literature, compounds exhibiting molar conductance values greater than 75 $S \cdot cm^2 \cdot mol^{-1}$ are typically considered electrolytic in nature. Therefore, the observed low conductivity values in this study further support the proposed neutral and non-ionic structures of the synthesized complexes.

Table 1 summarizes the physicochemical characteristics of the ligand (L) and its matching metal complexes.

Table 1. Physico-chemical characteristics of the ligand (L) and its complexes Cu(II), Zn(II) and Co(II).

Compound	W. (g/mol)	Yield (%)	Color	Λ (Scm_2mol^{-1})	M. P. (°C)
L	254.09	88	yellow	-	172
ZnL_2Cl_2	644	54	yellow	6.8	>300°C
CuL_2Cl_2	643	67	black	9.9	>300°C
$Co_2L_2(\mu\text{-}Cl)_2$	696	45	green	4.9	>300°C

3.2. UV-visible spectroscopy.

The electronic absorption spectra of the ligand (L) and its transition metal complexes (Figure 1) were recorded in 10^{-4} M DMF solutions at room temperature, within the 200–800 nm range. The corresponding electronic spectral data are summarized in Table 2. The UV–Vis spectrum of the free ligand (L) exhibits three absorption bands at approximately 309, 355, and 403 nm. The first two bands are attributed to π→π* transitions localized on the aromatic C=C bonds of the benzene rings, while the third, more intense band corresponds to an n→π* transition associated with the azomethine group, arising from the imine nitrogen atom's lone pair of electrons being excited to the C=N moiety's π* orbital [22]. In the spectra of the Cu(II), Zn(II), and Co(II) complexes, these bands appear with a slight bathochromic shift (≈4 nm), confirming the coordination of the ligand to the metal centers. Additionally, all complexes exhibit a broad absorption band in the visible region (500-700 nm), which can be assigned to d–d transitions characteristic of octahedral or square-planar metal coordination environments. Specifically, the Cu(II) complex exhibits a broad band centered around 543 nm, corresponding to the $^2B_1g \rightarrow {}^2E$ g transition, indicative of a square-planar geometry around the copper(II) ion [23]. The Co(II) complex shows two d-d bands at and 693 nm. These electronic transitions $^4A_1 \rightarrow {}^4B_1$ and $^4A_1 \rightarrow {}^4B_2$ indicate a tetrahedral geometry around Co(II) [24]. The diamagnetic complexes of the Zn^{2+} complex have a d10 system; thus, they do not show d-d transitions [25].

The electronic spectra clearly confirm the proposed geometries for the metal complexes. The appearance of d–d transitions in the Cu(II) and Co(II) complexes, and the absence of such bands in Zn(II), confirm the square-planar geometry for Cu(II) and the tetrahedral environment for Co(II) and Zn(II). The slight red or blue shifts of the ligand bands

during coordination further demonstrate the metal-ligand interaction. These results are consistent with ligand field theory and comparable to those reported for similar Schiff base complexes [21,23]. UV-Vis analysis, therefore, provides solid experimental evidence. The electronic spectra also confirm the proposed geometries. The Cu(II) complex exhibits a broad d-d transition around 543 nm, typical of a square planar geometry for a d^9 system. The Co(II) and Zn(II) complexes exhibit charge transfer bands consistent with tetrahedral environments. These observations are in perfect agreement with the coordination behavior inferred from the IR results.

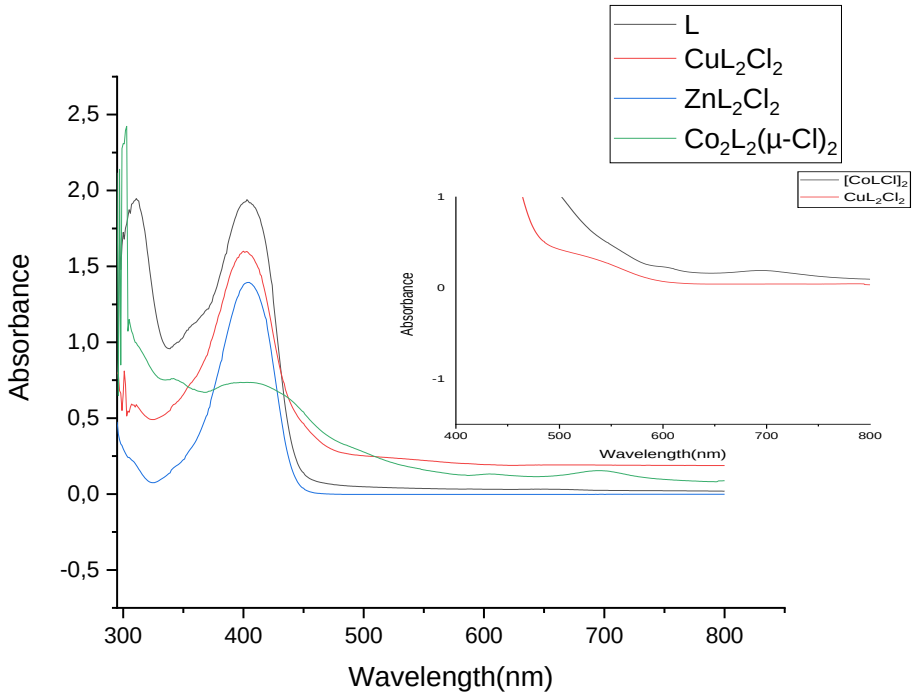

Figure 1. UV-Vis spectra of ligand **(L)** and its metal complexes Cu(II), Zn(II), and Co(II).

Table 2. UV-Vis absorption bands of (L) and its complexes Cu(II), Zn(II), and Co(II).

Compound	Bande	Electronic transition	Geometry
L	n→π*	403	-
	π →π*	309-355	
ZnL_2Cl_2	n→π*	308	Tetraedric
	π →π*	402	
CuL_2Cl_2	n→π*	401	Square plane
	π →π*	305	
	$^2Eg \leftarrow {}^2B_{1g}$	543	
$Co_2L_2(\mu\text{-}Cl)_2$	n→π*	399	Tetraedric
	π→π*	338	
	$^4A_1 \rightarrow {}^4B_1$ and $^4A_1 \rightarrow {}^4B_2$	601-692	

3.3. IR spectroscopy.

Infrared spectroscopy is one of the most informative techniques for elucidating the structural features of metal complexes. Comparing the IR spectra of the free ligand (L) with those of its corresponding complexes provides valuable insight into the functional groups involved in coordination and the internal vibrational modes of the molecules. The appearance or disappearance of characteristic absorption bands, as well as the shifting of existing bands, provides clear evidence of complex formation. Furthermore, IR spectra can reveal the presence of terminal and bridging M–Cl bonds by characteristic vibrational frequencies. The formation

of new absorption bands in the low-frequency region of the spectra corresponds to ν(M–O), ν(M–N), and ν(M–S) stretching vibrations, confirming metal–ligand coordination. A careful comparison between the spectra of the free ligand and its metal complexes shows appropriate shifts in key bands, supporting the involvement of specific donor atoms in complexation. The characteristic vibrational bands of ligand (L) and their shifts upon coordination are summarized in Table 3, while the corresponding IR spectra recorded in the 4000-400 cm^{-1} region are illustrated in Figure 2. The IR spectra of the ligand (L) and its metal complexes highlight the hydrocarbon framework through the presence of aromatic and aliphatic C–H stretching vibrations. Asymmetric and symmetric stretches of aromatic C–H are observed around 3000-3100 cm^{-1}, while aliphatic C–H (CH_3) stretching appears near 2900-3000 cm^{-1} in both the free ligand and the Zn(II), Co(II), and Cu(II) complexes. The free ligand exhibits a sharp and intense absorption band at 1611 cm^{-1}, characteristic of the azomethine (-C=N-) functional group. Upon complexation, this band shifts to lower wavenumbers, 1588 cm^{-1} for Zn(II), 1609 cm^{-1} for Cu(II), and 1608 cm^{-1} for Co(II), indicating coordination through the nitrogen atom of the azomethine group [26]. The aromatic C=C stretching vibrations are maintained at 1554 cm^{-1} in the free ligand, with shifts of 2-18 cm^{-1} observed in the corresponding metal complexes. The presence of the benzothiazole moiety is confirmed by the C–S stretching vibration at 621 cm^{-1} and the C–N stretching vibration at 1058 cm^{-1} in the ligand [27]. Furthermore, new bands appear in the complexes in the 452–480 cm^{-1} region, attributed to M–N stretching vibrations [28]. These observations confirm the coordination of the Schiff base ligand to the metal centers via the nitrogen of the azomethine group and, where relevant, the oxygen of the phenolic group [29].

IR spectral analysis clearly confirms the involvement of azomethine nitrogen in coordination, as evidenced by the shift of the ν(C=N) band to lower frequencies. The presence of new ν(M–N) bands between 452 and 480 cm^{-1} provides direct evidence of metal-nitrogen bonding.

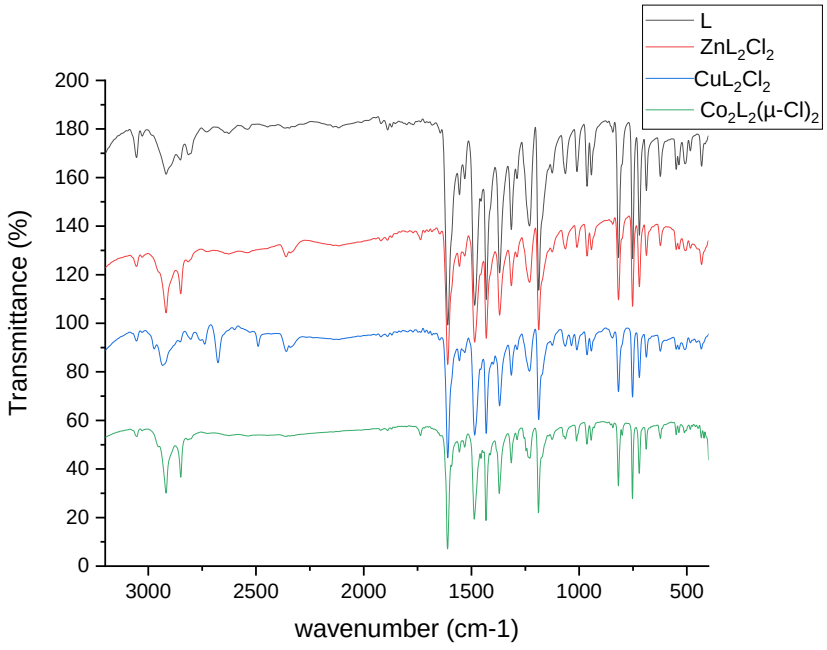

Figure 2. FTIR spectra of ligand (L) and its metal complexes Cu(II), Zn(II), and Co(II).

These results, combined with those from NMR and UV-Vis spectroscopy, demonstrate the formation of stable metal-ligand chelates. Similar vibrational shifts have been reported for

benzothiazole-based Schiff base complexes [14, 27], confirming the proposed coordination behavior.

Table 3. Main IR vibrational bands of the ligand (L) and its metal complexes Cu(II), Zn(II), and Co(II).

Compound	ν(C-H)	ν(C=N)	ν(C=C)	ν(C-N)	ν(C-S)	ν(M-N)
L	3059-2918	1612	1556	1058	621	-
ZnL_2Cl_2	3060-2959	1588	1572	1106	600	452
CuL_2Cl_2	3042-2915	1609	1552	1066	619	473
$Co_2L_2(\mu\text{-}Cl)_2$	3056-2924	1608	1559	1064	620	480

3.4. ^{1}H-NMR spectroscopy.

^{1}H-NMR spectroscopy was employed to investigate the coordination mode of the ligand to the central metal ions in the proposed M(II) complexes, complementing the findings from infrared spectroscopy (Scheme 3).

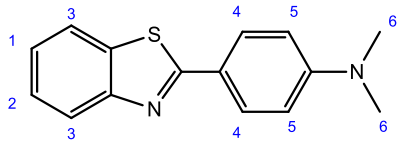

Scheme 3. Numbering order of the protons in the structure of the ligand (L).

In the ^{1}H-NMR spectrum of the free ligand (Figures S1 and S2), the eight aromatic protons are observed as two doublets (H3, H5), two triplets (H1, H2), and one doublet of doublets (H4). Similar splitting patterns can be appreciated in the spectra of the metal complexes (Figures S3-S7), albeit with slight shifts toward higher fields, indicative of coordination of the ligand to the metal centers. Specifically, the aromatic protons appear in the regions 8.00–6.77 ppm for Cu(II), 7.99-6.77 ppm for Zn(II), and 8.01–6.78 ppm for Co(II) (Table 4).

The aliphatic protons of the N-methyl groups (H6, –NCH_3) are observed at 2.98 ppm for the free ligand and at 2.97, 2.97, and 2.98 ppm for the Cu(II), Zn(II), and Co(II) complexes, respectively.

The slight upfield shifts of the aromatic proton signals upon complexation indicate alterations in the electronic environment caused by metal coordination. These changes demonstrate that the azomethine nitrogen (-CH=N–) is involved in attaching to the metal center. These observations are consistent with the IR spectral shifts of the ν(C=N) band and the UV-Vis electronic transitions, supporting the proposed square-planar geometry for the Cu(II) complex and tetrahedral geometries for the Zn(II) and Co(II) complexes.

Table 4. ^{1}H NMR spectral data of ligand(L) and its complexes.

Compound	δ(C-$H_{1\text{-}2\text{-}3\text{-}4\text{-}5}$) ppm	δ H_6(N-CH_3) ppm
L	7.98-6.78	2.98
CuL_2Cl_2	8.00-6.77	2.97
ZnL_2Cl_2	7.99-6.77	2.97
$Co_2L_2(\mu\text{-}Cl)_2$	8.01-6.78	2.98

3.5. ^{13}C-NMR spectroscopy.

The ^{13}C-NMR spectral data (Table 5) are consistent with the ^{1}H-NMR results and further confirm the proposed coordination mode of the ligand to the metal ions. In the spectrum of the free ligand (Figure S8), the signal observed at 168.39 ppm is assigned to the azomethine

carbon (–CH=N–). In the spectra of the metal complexes (Figures S9-S11), a slight shift of this signal to the range of 167.76-168.40 ppm is observed, demonstrating the azomethine nitrogen's coordination with the metal core.

Resonance signals appearing in the regions 154.54-112.42 ppm (for the free ligand) and 154.41-112.32 ppm (for the complexes) correspond to aromatic carbon atoms of the benzothiazole and phenyl rings. The aliphatic carbon signal of the N–CH_3 group is detected at 40.21 ppm for the free ligand and at 44.45, 40.44, and 40.48 ppm for the Zn(II), Cu(II), and Co(II) complexes, respectively [18].

The small downfield shifts of the imine and N–CH_3 carbon signals upon coordination provide additional confirmation of metal–ligand interaction through the azomethine nitrogen atom. These findings, together with the IR and ^{1}H-NMR data, strongly support the proposed coordination geometries of the synthesized complexes.

Table 5. ^{13}C NMR spectral data of Schiff base ligand and its complexes.

Compound	δ(H-C=N) ppm	δ(C-H$_{1-2-3-4-5}$) ppm	δ (N-CH$_3$) ppm
L	168.39	154.54-112.42	40.21
CuL_2Cl_2	167.76	152.74-112.32	40.44
ZnL_2Cl_2	168.40	154.41-112.32	40.45
$Co_2L_2(\mu\text{-}Cl)_2$	167.34	152.74-112.32	40.48

3.6. ESI-MS spectral analysis and structural correlation.

The molecular ion peaks of the ligand and its matching metal complexes were verified using electrospray ionization mass spectrometry (ESI-MS). There was a noticeable molecular ion peak in the free ligand's mass spectrum at *m/z* = 255 [M^+], along with fragment peaks at *m/z* = 241 and *m/z* = 225, attributed to $[C_{14}H_{11}N_2S]^+$ and $[C_{13}H_8N_2S]^+$, respectively (Scheme 4).

For the Cu(II) complex, the molecular ion peak appeared at *m/z* = 644 [M^+], while fragment peaks at *m/z* = 607, 576, and 571 correspond to successive fragmentations of the parent ion (Scheme 5). The Zn(II) complex displayed a distinct molecular ion peak at *m/z* = 645 [M^+]; additional peaks at *m/z* = 615 and *m/z* = 575 are attributed to the loss of two methyl groups and two chlorine atoms, respectively. Further fragmentation yielded a peak at *m/z* = 557 (elimination of $N_2C_2H_6$) and another at *m/z* = 531, corresponding to the loss of 2Cl and NCH_3 moieties.

The ESI-MS spectrum of the $Co_2L_2(\mu\text{–}Cl)_2$ complex showed a molecular ion peak at m/z = 697 [M^+], accompanied by characteristic fragment ions at *m/z* = 665 and *m/z* = 626, corresponding to the loss of two CH_3 groups and two chlorine atoms, respectively. The fragment at *m/z* = 655 can be assigned to the cleavage of the N-$(CH_3)_2$ group (Scheme 6).

The combined interpretation of the IR, UV-Vis, NMR, and ESI–MS data, together with molar conductance measurements, provides compelling evidence for the proposed coordination structures of the metal complexes. The downward shift of the azomethine (C=N) stretching band in the IR spectra confirms coordination through the imine nitrogen, consistent with the corresponding chemical shifts observed in the ^{1}H- and ^{13}C-NMR spectra. The UV-Vis spectra revealed d–d transition bands characteristic of square-planar geometry for the Cu(II) complex and tetrahedral geometry for the Zn(II) and Co(II) complexes.

Overall, the spectroscopic and analytical data collectively confirm the successful synthesis and structural integrity of the proposed Schiff base metal complexes, in agreement with similar systems previously reported in the literature [14,21,23].

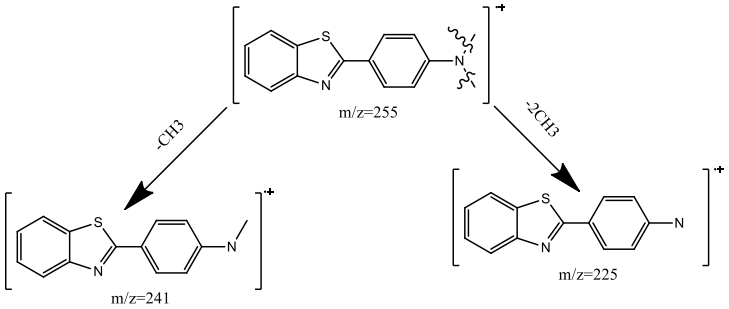

Scheme 4. Characteristic fragmentation of the ligand (**L**).

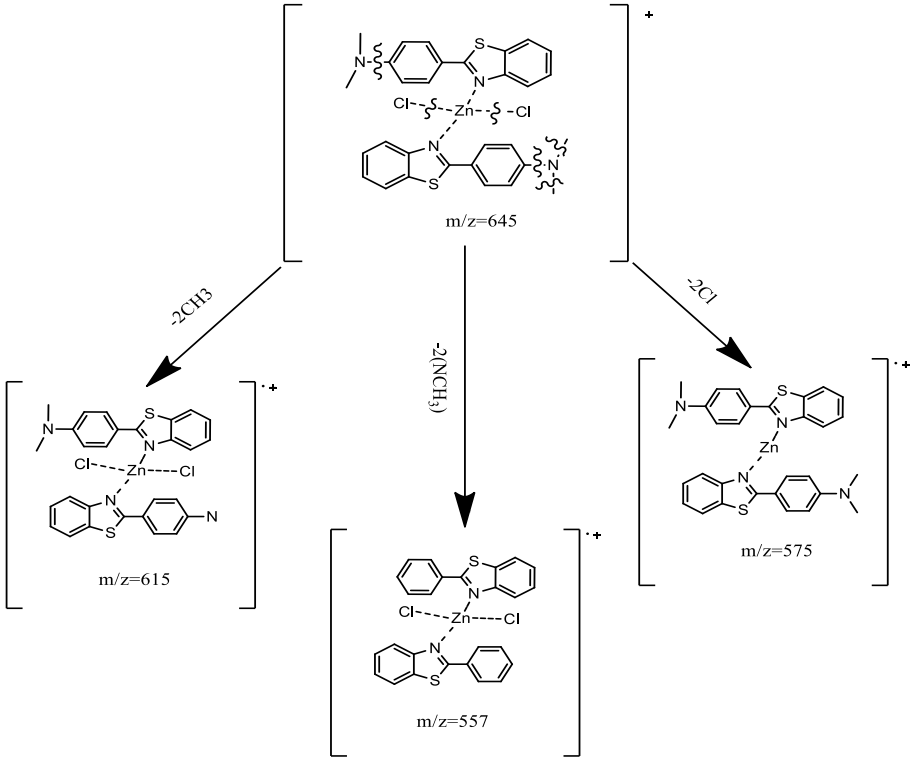

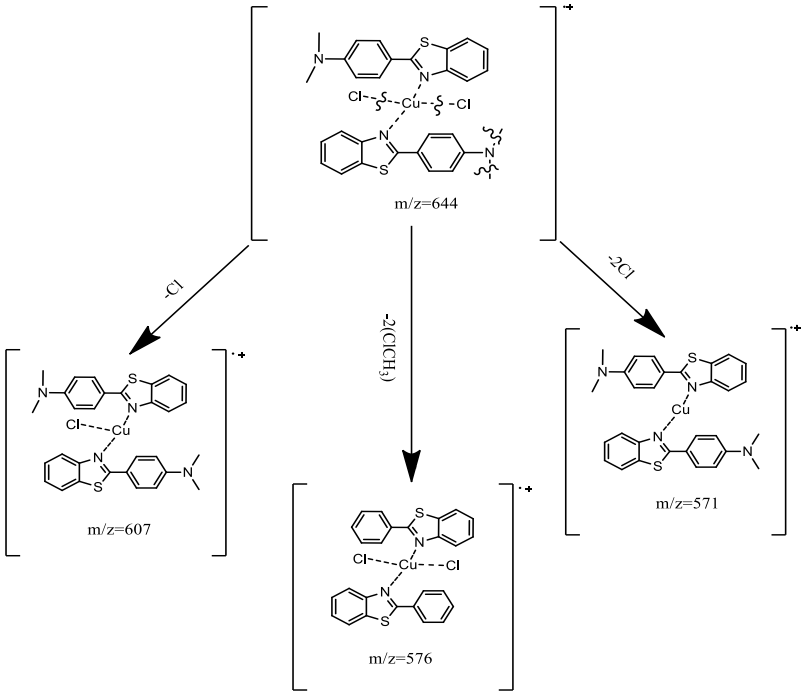

Scheme 5. Characteristic fragmentation of ZnL_2Cl_2 and CuL_2Cl_2 complexes.

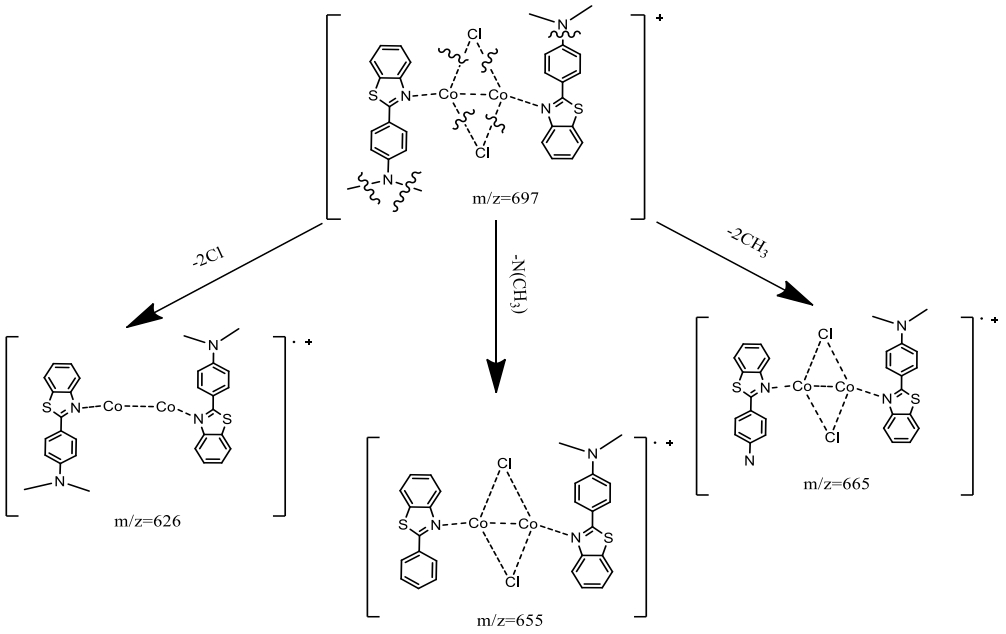

Scheme 6. Characteristic fragmentation of the complex $Co_2L_2(\mu\text{-}Cl)_2$.

3.7. Antioxidant activity.

Schiff bases and their transition metal complexes are known to exhibit significant antioxidant activity [30]. The antioxidant potential of organic ligands and their metal complexes depends on several factors, including the nature of the ligand (extent of conjugation and presence of radical-scavenging functional groups), geometry, ionization potential, reactivity, and reduction capacity [31]. Additionally, factors such as crystal structure, particle size, and morphology can influence the antioxidant efficiency of metal-containing compounds [32].

In this study, the DPPH radical scavenging experiment was used to systematically assess the antioxidant activity of the synthesized ligand (L) and its metal complexes, with L-ascorbic acid as a reference. The assay measures the ability of compounds to donate hydrogen atoms or electrons to neutralize the stable DPPH radical. Upon reduction, the DPPH solution changes color from purple to yellow, which was quantified by measuring the decrease in absorbance at 517 nm using a UV-Vis spectrophotometer (Figures 4-7). The IC_{50} values, representing the concentration required to scavenge 50% of DPPH radicals, are summarized in Figure 8 and Table 6. The results indicate the following trend in antioxidant activity: CuL_2Cl_2 > $Co_2L_2(\mu\text{–}Cl)_2$ > ZnL_2Cl_2 > L > ascorbic acid. Notably, compared to the free ligand, all metal complexes showed greater antioxidant activity, highlighting the effect of chelation on enhancing radical scavenging. The high activity of the free ligand is attributed to its structural features, which include several coordination sites such as the azomethine nitrogen (C=N), sulfur, and $N(CH_3)$ groups. These sites can participate in the antioxidant process by donating electrons or hydrogen [33]. However, complexation with metal ions further enhances activity by facilitating electron transfer and stabilizing radical intermediates [34]. Among the complexes, the Cu(II) derivative showed the highest antioxidant activity (IC_{50} = 0.008 mg/mL), which can be attributed to the redox potential of Cu^{2+} and its ability to act as a superoxide scavenging center. This redox property enhances the complex's electron-transfer capacity, accounting for its superior activity compared to Zn(II) and Co(II) analogs [35]. These findings

are in agreement with previous reports demonstrating enhanced antioxidant activity in Cu-Schiff base complexes relative to their free ligands [34].

Overall, the comparative evaluation of the ligand and its metal complexes indicates that metal chelation significantly improves antioxidant performance, supporting further in vivo studies to explore their pharmacological potential [27,36].

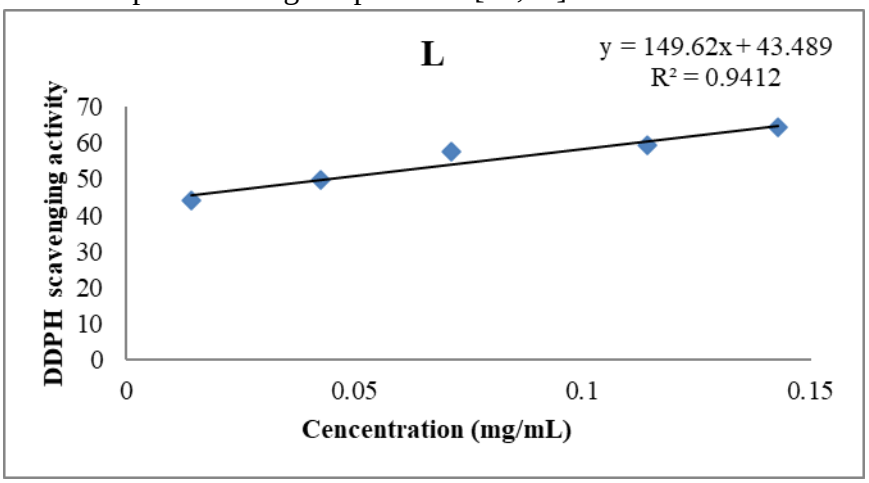

Figure 3. Antioxidant activity of ligand (**L**).

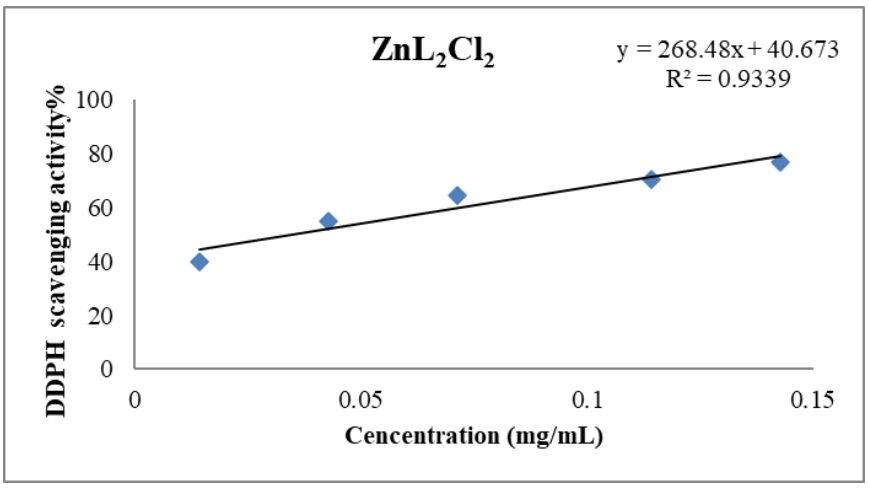

Figure 4. Antioxidant activity of the ZnL_2Cl_2 complex.

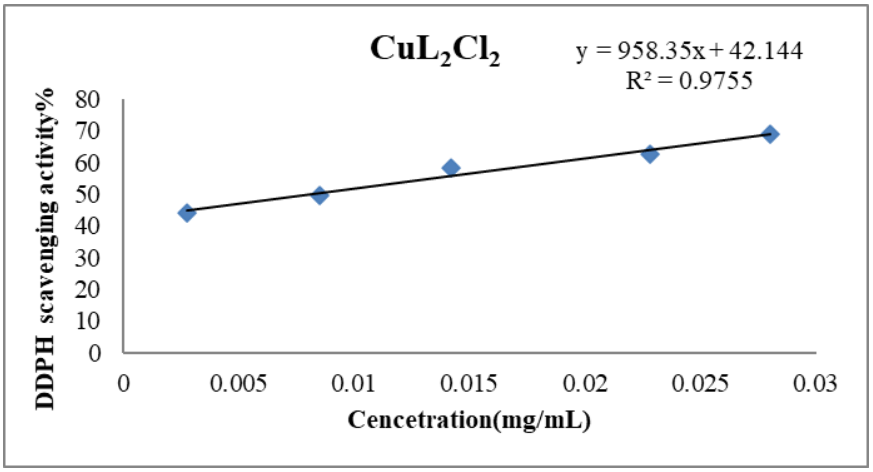

Figure 5. Antioxidant activity of the CuL_2Cl_2 complex.

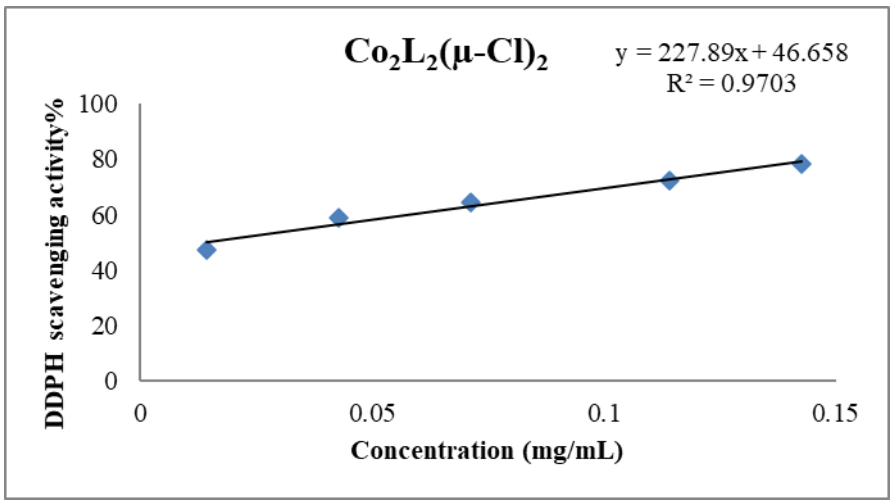

Figure 6. Antioxidant activity of the $Co_2L_2(\mu\text{-}Cl)_2$ complex.

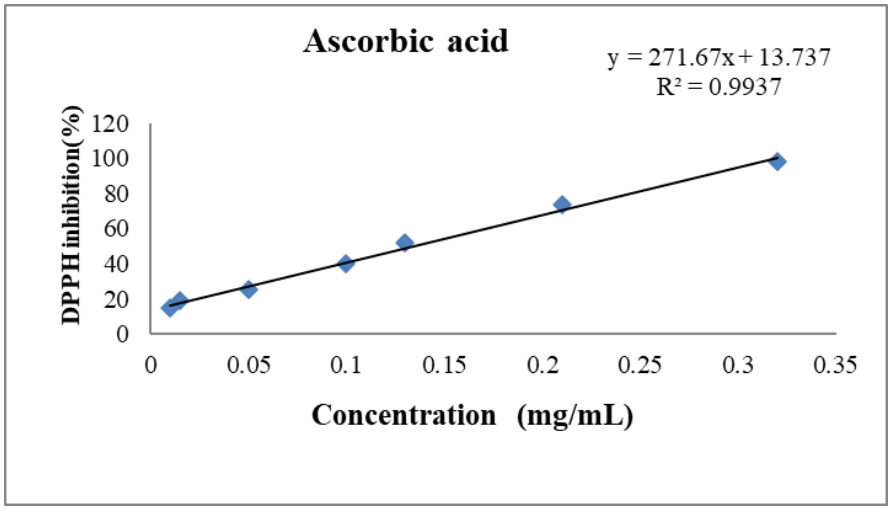

Figure 7. Antioxidant activity of ascorbic acid.

Table 6. IC_{50} values of the ligand (L) and its complexes Cu(II), Zn(II), and Co(II).

Compound	IC_{50}±SSD
L	0.043±0.004
ZnL_2Cl_2	0.024±0.007
CuL_2Cl_2	0.008±0.005
$Co_2L_2(\mu\text{-}Cl)_2$	0.014±0.003
Ascorbic acid	0.046±0.027

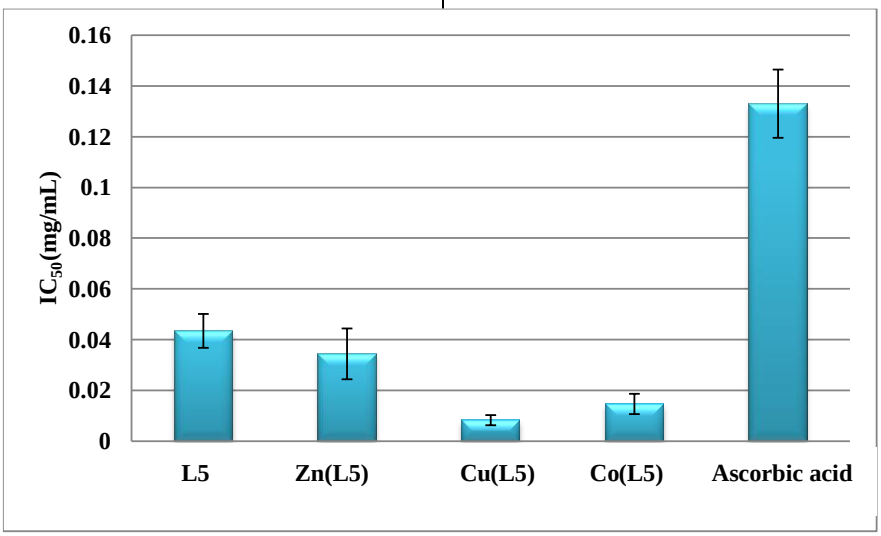

Figure 8. Inhibitory effect of the DPPH radical (IC_{50}) by the ligand L(L_5=L) and its complexes.

3.8. Antibacterial activity.

The antibacterial activity of the produced ligand and its metal complexes was assessed against four bacterial strains, and the results are summarized in Table 7. Among the tested compounds, *Pseudomonas aeruginosa* was the most susceptible. The $Co_2L_2(\mu–Cl)_2$ complex exhibited the strongest antibacterial activity, with MIC values of 0.078 mg/mL, 0.009 mg/mL, and 0.039 mg/mL against *Staphylococcus aureus*, *P. aeruginosa*, and *Escherichia coli*, respectively. In contrast, ZnL_2Cl_2 showed moderate activity against *E. coli* (MIC = 0.625 mg/mL), while the free ligand displayed no measurable antibacterial effect. These findings are consistent with previous reports indicating that metal chelates are generally more effective than their free ligands [37].

The observed variation in antibacterial efficacy can be attributed to differences in the structural and electronic properties of the complexes. The enhanced activity of the Co(II) complex is likely due to its optimal charge density and geometry, which improve chelation, reduce the metal ion's polarity, and increase lipophilicity, thereby facilitating stronger interactions with bacterial cell membranes.

According to the chelation theory, coordination enhances the metal ion's polarity by partially sharing its positive charge with ligand donor atoms and by delocalizing π-electrons over the chelate ring system. This reduction in polarity enhances the lipophilic character of the complex, promoting its penetration through the lipid-rich bacterial membrane [38]. Overtone's concept of cell permeability suggests that lipid membranes favor the passage of lipid-soluble substances; therefore, increased lipophilicity of the complexes directly enhances their antimicrobial activity [39].

Once inside the cell, these complexes may disrupt normal cellular processes by interfering with enzyme metal-binding sites, altering cell respiration, and inhibiting protein synthesis. Additionally, coordination via the azomethine nitrogen may enable hydrogen bonding with active centers of cellular constituents, further perturbing cellular function. The variation in activity against different microorganisms likely reflects differences in cell wall structure, ribosomal composition, and membrane permeability.

Overall, the study demonstrates that metal complexation significantly enhances antibacterial activity, particularly for Co(II) complexes, and supports their potential development as effective antimicrobial agents.

Table 7. Minimum inhibitory concentrations and the minimum bactericidal concentrations of ligand and its complexes (mg/mL).

Compound	*S. aureus*		*B. subtilis*		*P. aeruginosa*		*E. coli*	
	MIC	MBC	MIC	MBC	MIC	MBC	MIC	MBC
L	5.0±0.1	5.0±0.1	5.0±0.0	ND	5.0±0.1	5.0±0.0	5.0±0.1	5.0±0.0
CuL_2Cl_2	2.5±0.2	ND	5.0±0.1	ND	5.0±0.2	5.0±0.1	5.0±0.1	5.0±0.0
ZnL_2Cl_2	1.25±0.2	1.25±0.1	5.0±0.2	ND	5.0±0.1	ND	0.625±0.03	0.625±0.02
$Co_2L_2(\mu\text{-}Cl)_2$	0.078±0.002	0.078±0.001	0.625±0.001	ND	0.009±0.003	0.009±0.01	0.039±0.01	0.039±0.02

4. Conclusion

The ligand 4-(benzo[d]thiazol-2-yl)-N, N-dimethylaniline (L) and its corresponding Cu(II), Co(II), and Zn(II) complexes were successfully synthesized and structurally characterized using IR, UV–Visible, ^{1}H- and ^{13}C-NMR spectroscopy, mass spectrometry, and molar conductance measurements. Conductivity data indicated that all complexes are non-

electrolytic, while spectroscopic analyses confirmed coordination of the ligand to the metal center via the azomethine nitrogen. Structural elucidation suggests that the Cu(II) complex is mononuclear with a square-planar geometry (CuL_2Cl_2), the Zn(II) complex is mononuclear and tetrahedral (ZnL_2Cl_2), and the Co(II) complex is binuclear and tetrahedral ($Co_2L_2(\mu–Cl)_2$).

The antioxidant activity assessed by the DPPH radical scavenging method revealed that the ligand and its metal complexes exhibit substantial radical scavenging activity, surpassing that of the standard antioxidant ascorbic acid. Among the complexes, the Cu(II) derivative demonstrated the highest activity (IC_{50} = 0.0082 mg/mL), followed by Co(II) and Zn(II) complexes, highlighting the influence of metal coordination on enhancing antioxidant potential.

In vitro antibacterial studies showed that, compared to the free ligand, the metal complexes exhibited considerably greater activity against most tested microorganisms, with the Co(II) complex exhibiting the strongest antibacterial effect. These results confirm that coordination to transition metals modulates the electronic and structural properties of the Schiff base, leading to improved biological activities.

Overall, the combined spectroscopic and biological data validate the successful synthesis and functional relevance of these complexes. Future studies will focus on in vivo antioxidant evaluations, molecular interaction studies with DNA and proteins, and mechanistic investigations to better understand their pharmacological potential. These findings underscore the promising *in vitro* antioxidant and antibacterial properties of the synthesized complexes and provide a basis for further exploration of their biomedical applications.

Author Contributions

Conceptualization, I.E., A.B., and M.F.; methodology, I.E., S.E.R., and A.N.; software, I.E.; formal analysis, I.E., S.E.R., and A.B.; investigation, I.E., A.B., and M.F.; resources, I.E. and M.F.; data curation, I.E.; visualization, O.O., I.K.S., and N.E.M.; writing—original draft preparation, I.E. and S.E.R.; writing—review and editing, A.B., F.C., N.E.M., and M.F.; supervision, A.B., M.F., and F.C.; project administration, M.F. and F.C. All authors have read and agreed to the published version of the manuscript.

Institutional Review Board Statement

Not applicable.

Data Availability Statement

Data supporting the findings of this study are available upon reasonable request from the corresponding author.

Funding

This research received no external funding.

Conflicts of Interest

The authors declare no conflict of interest.

References

1. Paquin, F.; Rivnay, J.; Salleo, A.; Stingelin, N.; Silva, C. Multi-phase semicrystalline microstructures drive exciton dissociation in neat plastic semiconductors. *J. Mater. Chem. C* **2015**, *3*, 10715–10722, https://doi.org/10.1039/C5TC02043C.
2. Gill, R.K.; Rawal, R.K.; Bariwal, J. Recent advances in the chemistry and biology of benzothiazoles. *Arch. Pharm.* **2015**, *348*, 155–178, https://doi.org/10.1002/ardp.201400340.
3. Manoharan, D.; Thekkeppat, N.P.; Das, P.; Ghosh, S. Synthesis and characterisation of halogen substituted benzothiazole compounds. *Mater. Today Proc.* **2020**, *40*, S224–S229, https://doi.org/10.1016/j.matpr.2020.10.658.
4. Sharma, P.C.; Sinhmar, A.; Sharma, A.; Rajak, H.; Pathak, D.P. Medicinal significance of benzothiazole scaffold: An insight view. *J. Enzyme Inhib. Med. Chem.* **2012**, *28*, 240–266, https://doi.org/10.3109/14756366.2012.720572.
5. Yoshida, M.; Hayakawa, I.; Hayashi, N.; Agatsuma, T.; Oda, Y.; Tanzawa, F.; Iwasaki, S.; Koyama, K.; Furukawa, H.; Kurakata, S. Synthesis and biological evaluation of benzothiazole derivatives as potent antitumor agents. *Bioorg. Med. Chem. Lett.* **2005**, *15*, 3328-3332, https://doi.org/10.1016/j.bmcl.2005.05.077.
6. Keri, R.S.; Patil, M.R.; Patil, S.A.; Budagupi, S. A comprehensive review in current developments of benzothiazole-based molecules in medicinal chemistry. *Eur. J. Med. Chem.* **2015**, *89*, 207–251, https://doi.org/10.1016/j.ejmech.2014.10.059.
7. Meghdadi, S.; Amirnasr, M.; Mirhashemi, A.; Amiri, A. Synthesis, characterization and X-ray crystal structure of copper(I) complexes of the 2-(2-quinolyl)benzothiazole ligand. Electrochemical and antibacterial studies. *Polyhedron* **2015**, *97*, 234–239, https://doi.org/10.1016/j.poly.2015.05.026.
8. Su, X.; Vicker, N.; Ganeshapillai, D.; Smith, A.; Purohit, A.; Reed, M.J.; Potter, B.V. Benzothiazole derivatives as novel inhibitors of human 11β-hydroxysteroid dehydrogenase type 1. *Mol. Cell. Endocrinol.* **2006**, *248*, 214-217, https://doi.org/10.1016/j.mce.2005.10.022.
9. Cressier, D.; Prouillac, C.; Hernandez, P.; Amourette, C.; Diserbo, M.; Lion, C.; Rima, G. Synthesis, antioxidant properties and radioprotective effects of new benzothiazoles and thiadiazoles. *Bioorg. Med. Chem.* **2009**, *17*, 5275-5284, https://doi.org/10.1016/j.bmc.2009.05.039.
10. Doğruer, D.S.; Ünlü, S.; Şahin, M.F.; Yeşilada, E. Anti-nociceptive and anti-inflammatory activity of some (2-benzoxazolone-3-yl and 2-benzothiazolone-3-yl)acetic acid derivatives. *Farmaco* **1999**, *53*, 80–84, https://doi.org/10.1016/s0014-827x(97)00017-7.
11. Jena, J. Significance of benzothiazole moiety in the field of cancer. *Int. J. Pharm. Pharm. Sci.* **2014**, *6*, 16–22.
12. Kiran, T.; Pathak, M.; Chanda, K.; Balamurali, M.M. DNA and protein interaction studies of heteroleptic copper(II) derivatives of benzothiazole-based Schiff base and N,N-donor ligands. *ChemistrySelect* **2020**, *5*, 6792–6799, https://doi.org/10.1002/slct.202001246.
13. Karegoudar, P.; Karthikeyan, M.S.; Prasad, D.J.; Mahalinga, M.; Holla, B.S.; Kumari, N.S. Synthesis of some novel 2, 4-disubstituted thiazoles as possible antimicrobial agents. *Eur. J. Med. Chem.* **2008**, *43*, 261-267, https://doi.org/10.1016/j.ejmech.2007.03.014.
14. Mishra, N.; Gound, S.S.; Mondal, R.; Yadav, R.; Pandey, R. Synthesis, characterization and antimicrobial activities of benzothiazole-imino-benzoic acid ligands and their Co(II), Ni(II), Cu(II), Zn(II) and Cd(II) complexes. *Results Chem.* **2019**, *1*, 100006, https://doi.org/10.1016/j.rechem.2019.100006.
15. Chen, G.-J.; Qiao, X.; Qiao, P.-Q.; Xu, G.-J.; Xu, J.-Y.; Tian, J.-L.; Gu, W.; Liu, X.; Yan, S.-P. Synthesis, DNA binding, photo-induced DNA cleavage, cytotoxicity and apoptosis studies of copper (II) complexes. *J. Inorg. Biochem.* **2011**, *105*, 119-126, https://doi.org/10.1016/j.jinorgbio.2010.11.008.
16. Chand, D.K.; Schneider, H.J.; Bencini, A.; Bianchi, A.; Giorgi, C.; Ciattini, S.; Valtancoli, B. Affinity and nuclease activity of macrocyclic polyamines and their CuII complexes. *Chem. Eur. J.* **2000**, *6*, 4001-4008, https://doi.org/10.1002/1521-3765(20001103)6:21%3C4001::aid-chem4001%3E3.3.co;2-i.
17. Harinath, Y.; Kumar, D.H.; Kumar, B.N.; Apparao, C.; Seshaiah, K. Synthesis, spectral characterization and antioxidant activity studies of a bidentate Schiff base, 5-methyl thiophene-2-carboxaldehyde-carbohydrazone and its Cd(II), Cu(II), Ni(II) complexes. *Spectrochim. Acta A Mol. Biomol. Spectrosc.* **2013**, *101*, 264–272, https://doi.org/10.1016/j.saa.2012.09.085.

18. Nawaz, N.; Ahmad, I.; Darwesh, N.M.; Wahab, A.; Rahman, S.U.; Sajid, A.; Khan, F.A.; Khan, S.B.; Patching, S.G.; Uddin, K. Synthesis, characterization and antioxidant activity of nickel (II) Schiff base complexes derived from 4-(dimethylamino) benzaldehyde. *J. Chem. Soc. Pak.* **2020**, *42*, 238-242.
19. Lopes-Lutz, D.; Alviano, D.S.; Alviano, C.S.; Kolodziejczyk, P.P. Screening of chemical composition, antimicrobial and antioxidant activities of Artemisia essential oils. *Phytochemistry* **2008**, *69*, 1732–1738, https://doi.org/10.1016/j.phytochem.2008.02.014.
20. Elaaraj, I.; Raouan, S.E.; Nakkabi, A.; Es-sounni, B.; Koraichi, I.; Fahim, M. Synthesis, characterization and antioxidant, antibacterial activity Zn^{2+}, Cu^{2+}, Ni^{2+} and Co^{2+}, complexes of ligand [2-(thiophen-2-yl)-1-(thiophen-2-ylmethyl)-1H-benzo [d] imidazole]. *J. Indian Chem. Soc.* **2022**, *99*, 100404, https://doi.org/10.1016/j.jics.2022.100404.
21. Venkateswarlu, K.; Pradeep, M.; Rambabu, A. Crystal structure, DNA binding, cleavage, antioxidant and antibacterial studies of Cu(II), Ni(II) and Co(III) complexes with 2-((furan-2-yl)methylimino)methyl)-6-ethoxyphenol Schiff base. *J. Mol. Struct.* **2018**, *1160*, 198–207, https://doi.org/10.1016/j.molstruc.2018.02.004.
22. Ganji, N.; Rambabu, A.; Vamsikrishna, N.; Daravath, S. Copper(II) complexes with isoxazole Schiff bases: Synthesis, spectroscopic investigation, DNA binding and nuclease activities, antioxidant and antimicrobial studies. *J. Mol. Struct.* **2018**, *1173*, 173–182, https://doi.org/10.1016/j.molstruc.2018.06.100.
23. Ramesh, G.; Daravath, S.; Ganji, N.; Rambabu, A.; Venkateswarlu, K. Facile synthesis, structural characterization, DNA binding, incision evaluation, antioxidant and antimicrobial activity studies of Cobalt (II), Nickel (II) and Copper (II) complexes of 3-amino-5-(4-fluorophenyl) isoxazole derivatives. *J. Mol. Struct.* **2020**, *1202*, 127338, https://doi.org/10.1016/j.molstruc.2019.127338.
24. Shaygan, S.; Pasdar, H.; Foroughifar, N.; Davallo, M.; Motiee, F. Cobalt(II) complexes with Schiff base ligands derived from terephthalaldehyde and ortho-substituted anilines: Synthesis, characterization and antibacterial activity. *Appl. Sci.* **2018**, *8*, 385, https://doi.org/10.3390/app8030385.
25. Shakdofa, M.M.E.; Al-Hakimi, A.N.; Elsaied, F.A.; Alasbahi, S.O.M.; Alkwlini, A.M.A. Synthesis, characterization and bioactivity of Zn^{2+}, Cu^{2+}, Ni^{2+}, Co^{2+}, Mn^{2+}, Fe^{3+}, Ru^{3+}, VO^{2+} and UO_2^{2+} complexes of 2-hydroxy-5-((4-nitrophenyl)diazenyl)benzylidene)-2-(p-tolylamino)acetohydrazide. *Bull. Chem. Soc. Ethiop.* **2017**, *31*, 75–91, https://doi.org/10.4314/bcse.v31i1.7.
26. Rambabu, A.; Kumar, M.P.; Tejaswi, S.; Vamsikrishna, N. DNA interaction and antimicrobial studies of newly synthesized copper(II) complexes with 2-amino-6-(trifluoromethoxy)benzothiazole Schiff base ligands. *J. Photochem. Photobiol. B Biol.* **2016**, *165*, 147–156, https://10.1016/j.jphotobiol.2016.10.027.
27. Elaaraj, I.; Bouymajane, A.; Raouan, S.E.; Nakkabi, A.; Oulidi, O.; Filali, F.R.; Cacciola, F.; El Moualij, N.; Fahim, M. Synthesis, characterization and biological studies of novel copper(II) and Ni(II) complexes and triphenylphosphine. *Viet. J. Chem.* **2024**, *62*, 527-539, https://doi.org/10.1002/vjch.202300242.
28. Zehra, S.; Khan, M.S.; Ahmad, I.; Arjmand, F. New tailored substituted benzothiazole Schiff base Cu(II)/Zn(II) antitumor drug entities: Effect of substituents on DNA binding profile, antimicrobial and cytotoxic activity. *J. Biomol. Struct. Dyn.* **2018**, *37*, 1863-1879,. https://doi.org/10.1080/07391102.2018.1467794.
29. Elaaraj, I.; Driouch, M.; Kadiri, M.; Safi, Z.; Nakkabi, A.; Oulidi, O.; El Moualij, N.; Benhiba, F.; Fahim, M.; Haoudi, A. Synthesis, Characterization, and Corrosion Inhibition Assessment of Three New Mononuclear Hybrid Complexes Based on Schiff (2-(2-Hydroxybenzylidene) amino) phenol and Triphenylphosphine Ligand. *ACS Omega* **2025**, *10*, 38359-38375, https://doi.org/10.1021/acsomega.4c04380.
30. Nitha, L.P.; Aswathy, R.; Elsa, N.; Sindhu, B.; Mohanan, K. Synthesis, spectroscopic characterisation, DNA cleavage, superoxidase dismutase activity and antibacterial properties of some transition metal complexes of a novel bidentate Schiff base derived from isatin and 2-aminopyrimidine. *Spectrochim. Acta A Mol. Biomol. Spectrosc.* **2014**, *118*, 154–161, https://doi.org/10.1016/j.saa.2013.08.075.
31. Nami, S.A.A.; Alam, M.; Husain, A.; Parveen, M. Synthesis, characterization, thermal and antioxidant studies of potassium dihydrobisphenothiazinyl borate and its transition metal complexes. *Spectrochim. Acta A Mol. Biomol. Spectrosc.* **2012**, *96*, 729–735, https://doi.org/10.1016/j.saa.2012.07.033.
32. Ilies, D.; Shova, S.; Radulescu, V.; Pahontu, E.; Rosu, T. Synthesis, characterization, crystal structure and antioxidant activity of Ni(II) and Cu(II) complexes with 2-formilpyridine N(4)-phenylthiosemicarbazone. *Polyhedron* **2015**, *97*, 157–166, https://doi.org/10.1016/j.poly.2015.05.009.
33. Panhwar, Q.K.; Memon, Synthesis, characterisation, and antioxidant study of Cr(III)-rutin complex. *Chem.*

Pap. **2014**, *68*, 614–623, https://doi.org/10.2478/s11696-013-0494-6.
34. Shakir, M.; Hanif, S.; Sherwani, M.A.; Mohammad, O.; Al-Resayes, S.I. Pharmacologically significant complexes of Mn(II), Co(II), Ni(II), Cu(II) and Zn(II) of novel Schiff base ligand (E)-N-(furan-2-ylmethylene)quinolin-8-amine: Synthesis, spectral, XRD, SEM, antimicrobial, antioxidant and *in vitro* cytotoxic studies. *J. Mol. Struct.* **2015**, *1092*, 143–159, https://doi.org/10.1016/j.molstruc.2015.03.012.
35. Saif, M.; El-Shafiy, H. F.; Mashaly, M.M.; Eid, M.F.; Nabeel, A.I.; Fouad, R.Synthesis, characterization, and antioxidant/cytotoxic activity of new chromone Schiff base nano-complexes of Zn(II), Cu(II), Ni(II) and Co(II). *J. Mol. Struct.* **2016**, *1118*, 75–82, https://doi.org/10.1016/j.molstruc.2016.03.060.
36. Rana, M.S.; Rayhan, N.M.A.; Emon, M.S.H.; Islam, M.T.; Rathry, K.; Hasan, M.M.; Mansur, M.M.I.; Srijon, B.C.; Islam, M.S.; Ray, A. Antioxidant activity of Schiff base ligands using the DPPH scavenging assay: an updated review. *RSC Adv.* **2024**, *14*, 33094-33123, https://doi.org/10.1039/D4RA04375H.
37. Kargar, H.; Adabi, A.; Nawaz, M.; Ashfaq, M.; Shahzad, K. Synthesis, spectral characterization, crystal structure and antibacterial activity of nickel(II), copper(II) and zinc(II) complexes containing ONNO donor Schiff base ligands. *J. Mol. Struct.* **2021**, *1233*, 130112, https://doi.org/10.1016/j.molstruc.2021.130112.
38. Venkateswarlu, K.; Pradeep, M.; Rambabu, A. Crystal structure, DNA binding, cleavage, antioxidant and antibacterial studies of Cu (II), Ni (II) and Co (III) complexes with 2- ((furan-2-yl) methylimino) methyl) -6-ethoxyphenol Schiff base. *J. Mol. Struct.* **2018**, *1160*, 198–207, https://doi.org/10.1016/j.molstruc.2018.02.004.
39. Daravath, S.; Rambabu, A.; Shankar, D.S. Structure elucidation of copper (II), cobalt (II) and nickel (II) complexes of benzothiazole derivatives: Investigation of DNA binding, nuclease efficacy, free radical scavenging and biocidal properties. *Chem. Data Collect.* **2019**, *24*, 100293, https://doi.org/10.1016/j.cdc.2019.100293.

Publisher's Note & Disclaimer

Supplementary materials

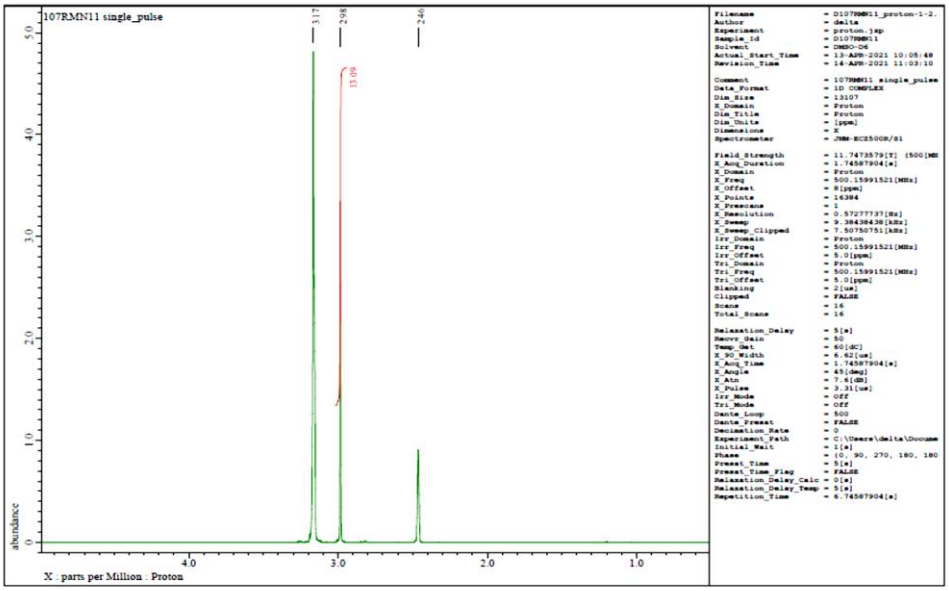

Figure S1. ^{1}H NMR spectrum of the ligand (L).

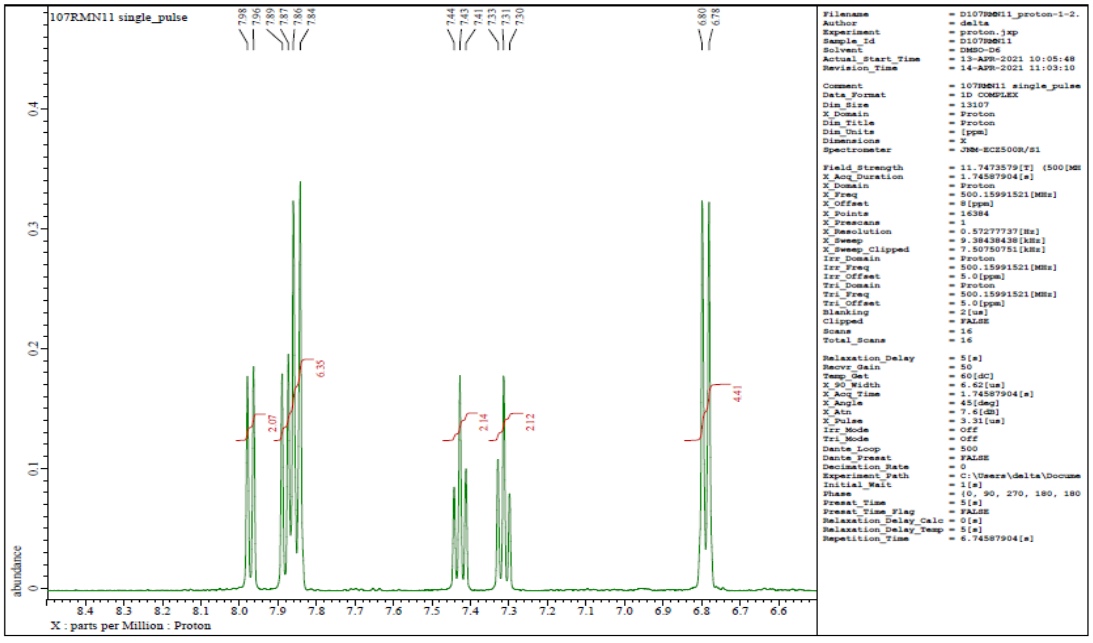

Figure S2. ^{1}H NMR spectrum of the ligand (L).

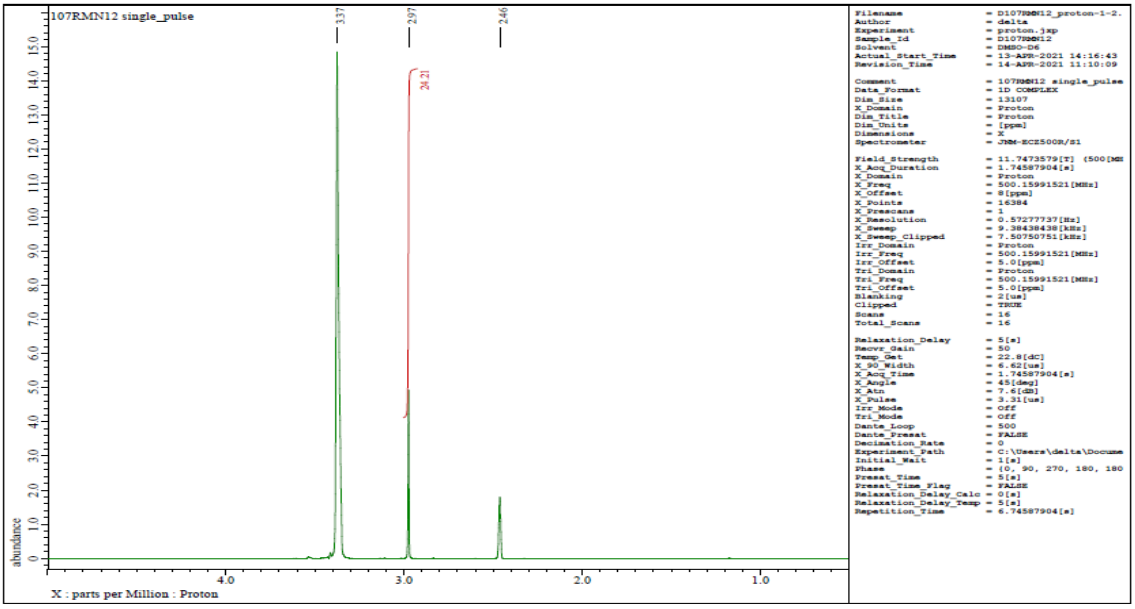

Figure S3. ^{1}H NMR spectrum of the complex ZnL_2Cl_2.

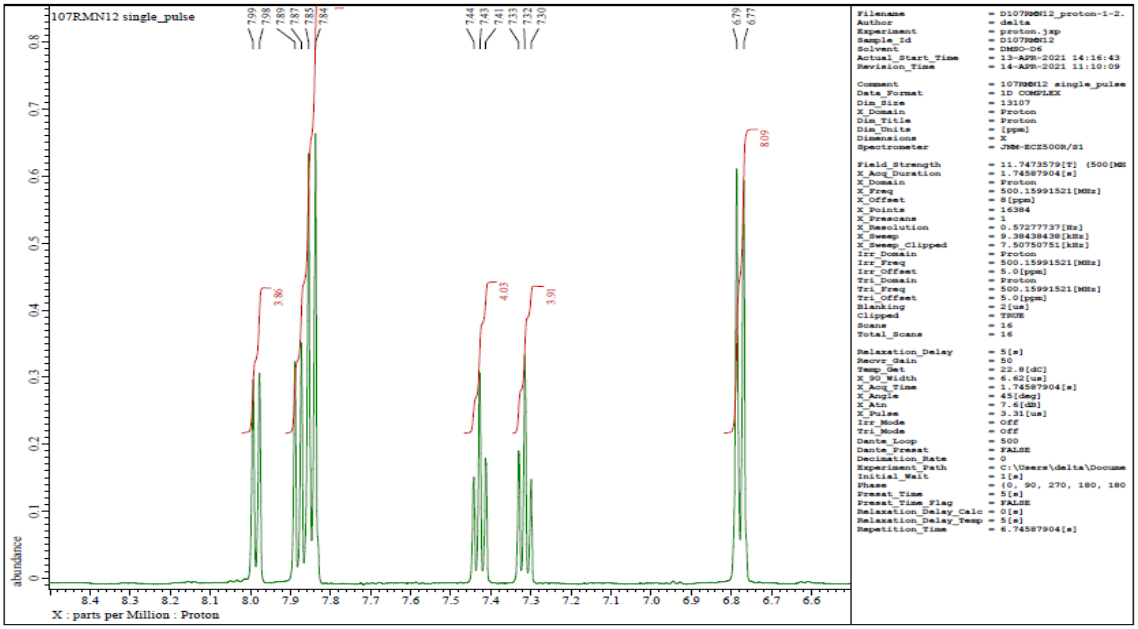

Figure S4.^{1}H NMR spectrum of the complex ZnL_2Cl_2.

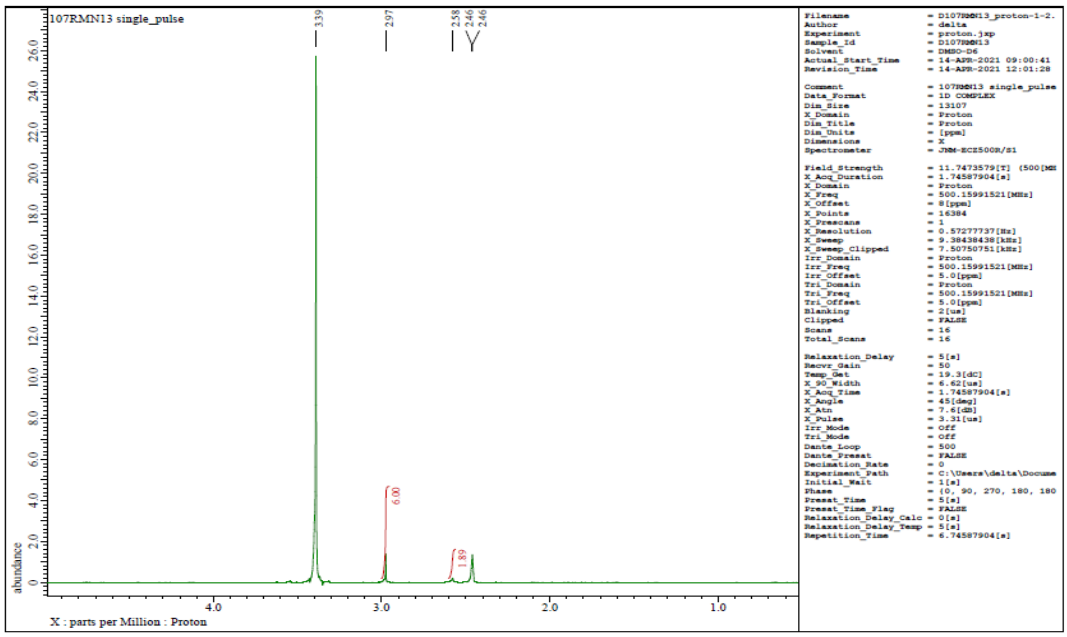

Figure S5. ^{1}H NMR spectrum of the complex CuL_2Cl_2.

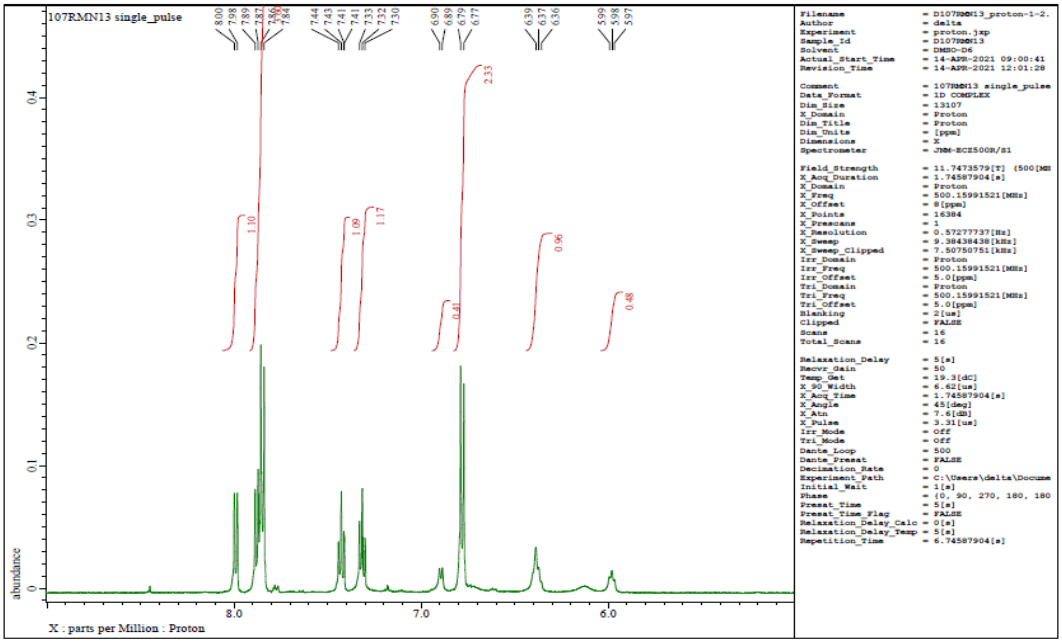

Figure S6. ^{1}H NMR spectrum of the complex CuL_2Cl_2.

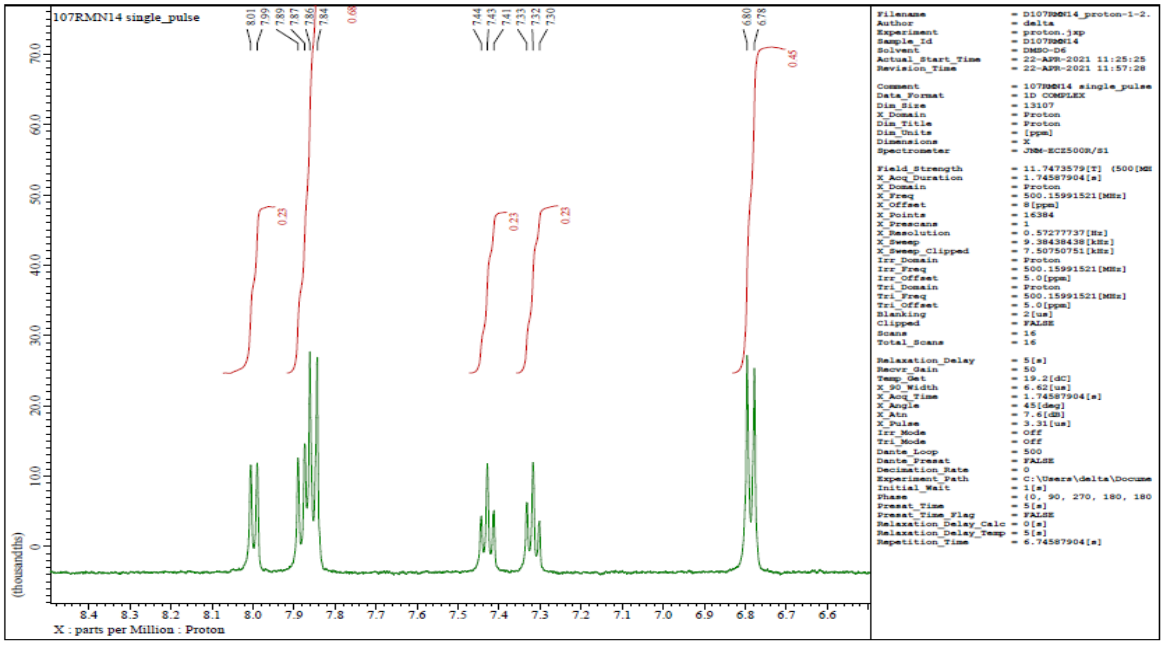

Figure S7. [1]H NMR spectrum of the complex $Co_2L_2(\mu\text{-}Cl)_2$.

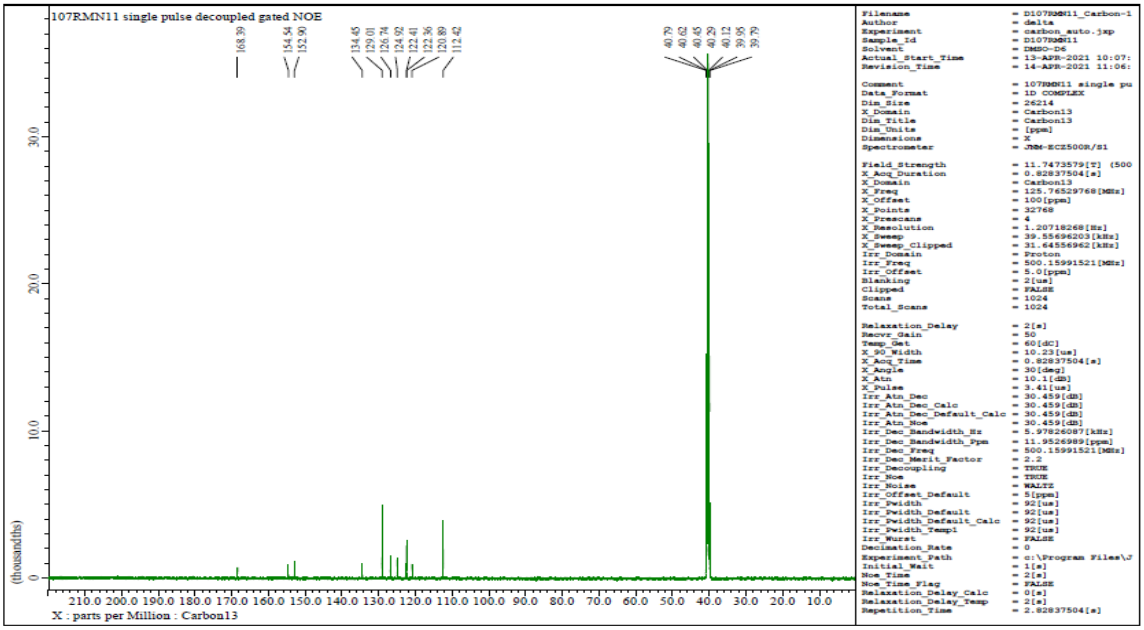

Figure S8. [13]C NMR spectrum of the ligand (L).

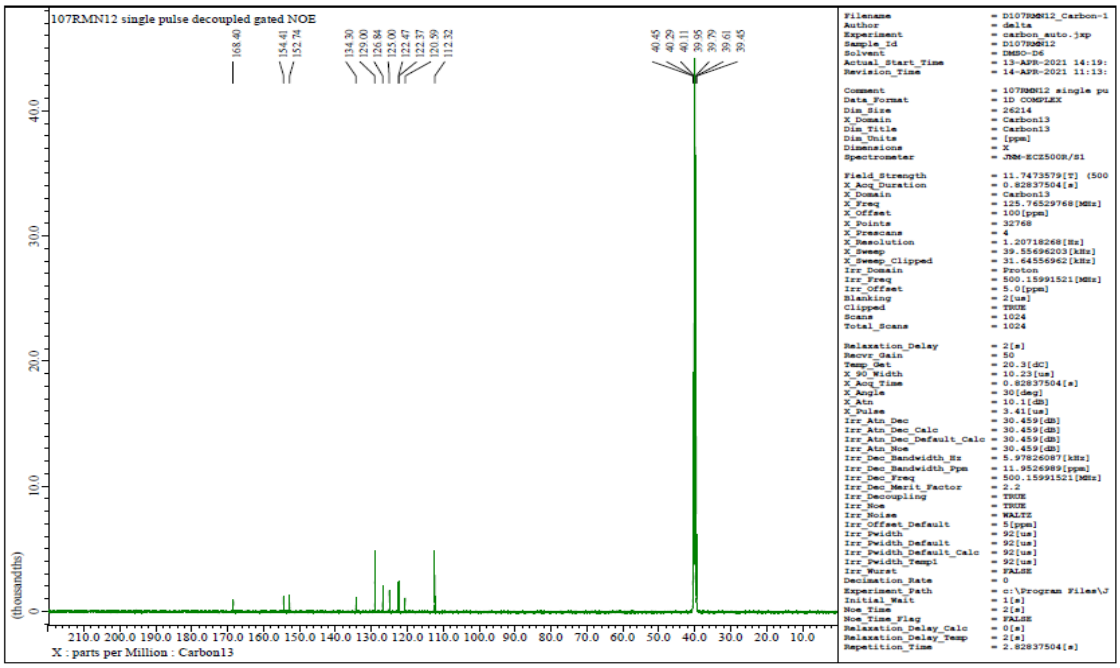

Figure S9. ^{13}C NMR spectrum of the complex ZnL_2Cl_2.

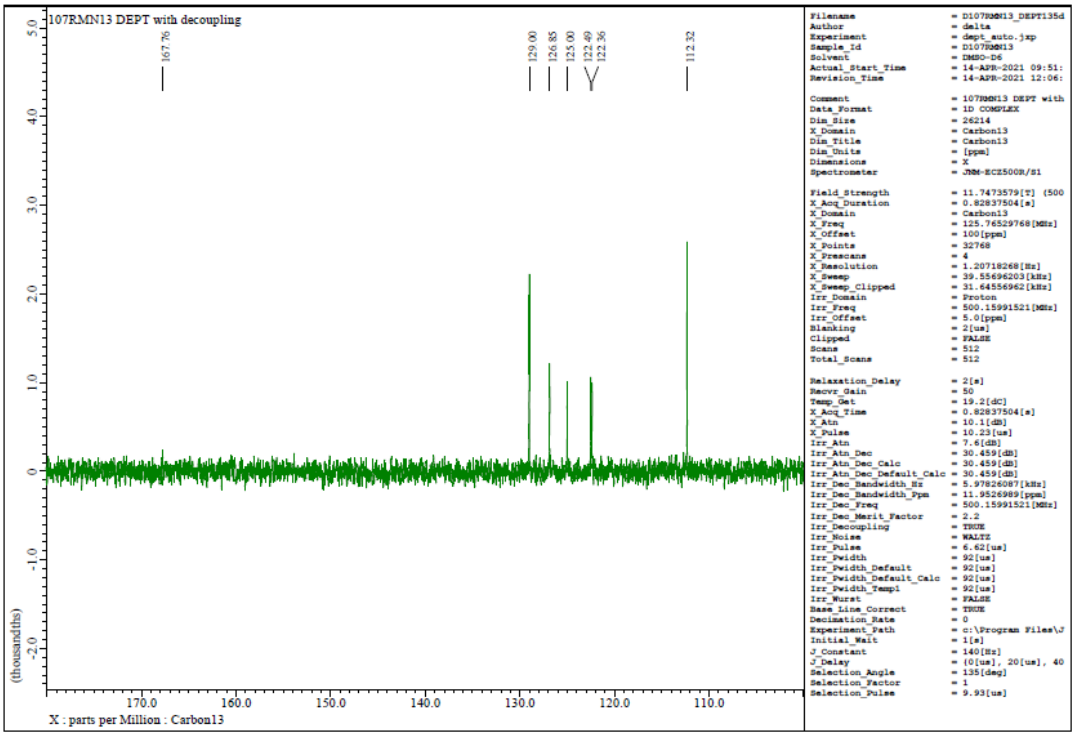

Figure S10. ^{13}C NMR spectrum of the CuL_2Cl_2.

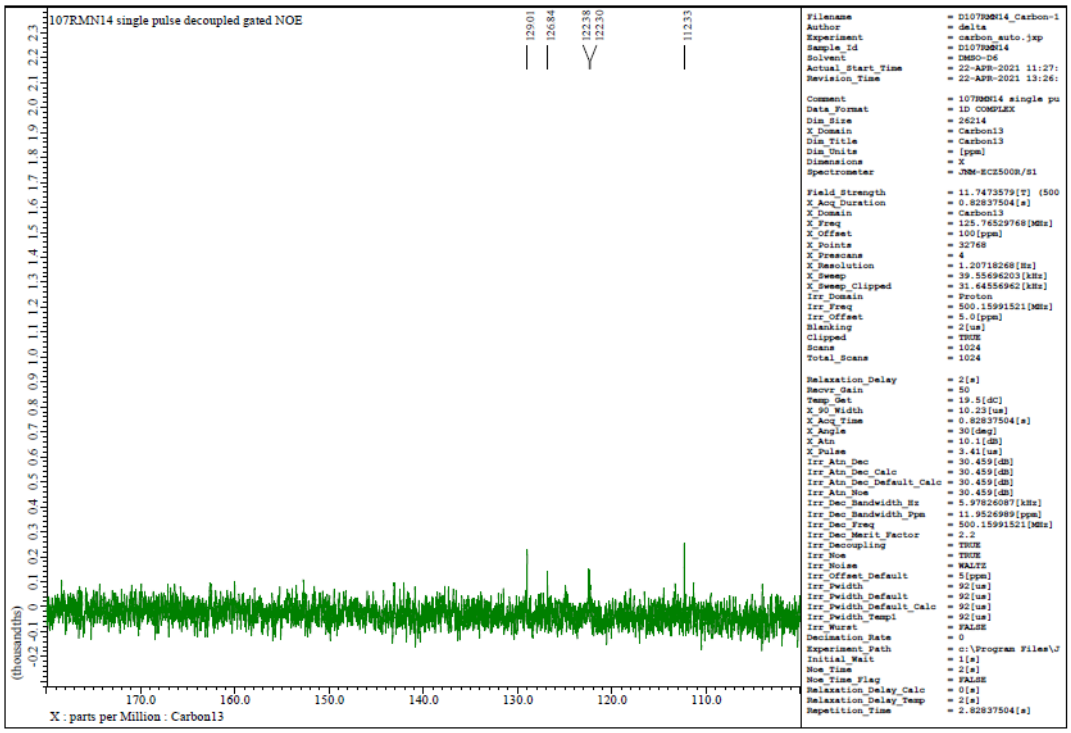

Figure S11. ^{13}C NMR spectrum of the complex $Co_2L_2(\mu\text{-}Cl)_2$.